

## Supporting Information Appendix

# **Binding site for coenzyme A revealed in the structure of pyruvate:ferredoxin oxidoreducatase from *Moorella thermoacetica***

Percival Yang-Ting Chen<sup>a</sup>, Heather Aman<sup>b</sup>, Mehmet Can<sup>b</sup>, Stephen W. Ragsdale<sup>b</sup>, Catherine L. Drennan<sup>a,c,d</sup>

<sup>a</sup>Department of Chemistry, <sup>c</sup>Department of Biology, and <sup>d</sup>Howard Hughes Medical Institute, Massachusetts Institute of Technology, Cambridge, MA 02139, United States

<sup>b</sup>Department of Biological Chemistry, University of Michigan, Ann Arbor, Michigan 48109, United States

**SI Appendix – Materials and Methods**

**SI Appendix – Figures S1-S11**

**SI Appendix – Tables S1-S4**

**SI Appendix – References**

**SI Appendix – Materials and Methods**

**Protein purification and activity.** *Moorella thermoacetica* growth, enzyme isolation and protein quantification were performed as described previously (1). However, in the purification protocol, Tris-HCl buffer at pH 7.6 was used instead of MOPS. Enzyme quality was assessed by sodium dodecyl sulfate-polyacrylamide gel electrophoresis (SDS-PAGE) and enzyme activity assays. Enzyme assays were conducted at 20 °C in 50 mM Tris-HCl buffer at pH 7.6 including 2 mM DTT, 1 mM TPP, 1 mM MgCl<sub>2</sub>, 1 mM Coenzyme A hydrate, 10 mM sodium pyruvate, and 10 mM oxidized methyl viologen. The assay was started by adding PFOR and the absorbance at 578 nm of reduced methyl viologen was followed as a function of time. Activities of the different preparations of enzyme used in this study appeared homogeneous by SDS-PAGE analyses and exhibited pyruvate oxidoreductase activities of 8.3, 12.0, and 13.8 μmol pyruvate oxidized min<sup>-1</sup> mg<sup>-1</sup>.

**Crystallization of native *MtPFOR* and pyruvate soaking experiment.** *MtPFOR* was crystallized by sitting drop crystallization method in a Coy anaerobic chamber with an Ar/H<sub>2</sub> environment at room temperature. Brown plate crystals grew within 4-7 days of mixing 1.5 μL of 6.2 mg/mL *MtPFOR* in storage buffer (50 mM Tris pH 7.5, 1 mM TPP (Sigma-Aldrich), and 1 mM MgCl<sub>2</sub>) with 0.5 μL well solution (15-16% (w/v) PEG 4000, 0.21 M (NH<sub>4</sub>)<sub>2</sub>SO<sub>4</sub>, and 0.10 M MES pH 6.0) to make a 2.0 μL sitting drop in a sealed well with 500 μL well solution. The crystal used to determine the native structure was transferred to cryoprotectant (20% (v/v) glycerol, 20% (w/v) PEG 4000, 0.07 M (NH<sub>4</sub>)<sub>2</sub>SO<sub>4</sub>, and 0.10 M MES pH 6.0) briefly and flash-cooled in liquid nitrogen. The crystals used in pyruvate soaking experiments were transferred into cryoprotectant (20% (v/v) glycerol, 20% (w/v) PEG 4000, 0.18 M (NH<sub>4</sub>)<sub>2</sub>SO<sub>4</sub>, 0.10 M MES pH 6.0, and 50 mM pyruvate (Sigma-Aldrich)) for 15 mins or 12 hrs and flash-cooled in liquid nitrogen. All the chemicals, unless stated otherwise, are from Hampton Research. The native *MtPFOR* and pyruvate-soaked PFOR crystals formed in the space group C2 with unit cell constants  $a = 340 \text{ \AA}$ ,  $b = 108 \text{ \AA}$ , and  $c = 240 \text{ \AA}$ ,  $\beta = 109^\circ$ .

**Cocrystallization of *MtPFOR* with coenzyme A.** *MtPFOR* was crystallized with CoA in a Coy anaerobic chamber with an Ar/H<sub>2</sub> environment at room temperature using the sitting drop crystallization method. Brown plate crystals grew within 7 days of mixing 1.5 μL of 5.2 mg/mL *MtPFOR* in storage buffer with coenzyme A (50 mM Tris pH 7.5, 1 mM TPP (Sigma-Aldrich), 1 mM MgCl<sub>2</sub>, and 10 mM CoA (Sigma-Aldrich)) with 0.5 μL

well solution (13% (w/v) PEG 6000 and 0.06 M sodium cacodylate pH 6.5) to make a 2.0  $\mu$ L sitting drop in a sealed well with 500  $\mu$ L of well solution. The crystal used to determine the CoA cocrystal structure was briefly soaked into a cryoprotectant (10 mM CoA (Sigma-Aldrich), 15% (w/v) PEG 6000, and 20% (v/v) glycerol) and flash-cooled in liquid nitrogen. All the chemicals, unless stated otherwise, are from Hampton Research. Crystals formed in space group *C*2 with unit cell constants  $a = 338 \text{ \AA}$ ,  $b = 107 \text{ \AA}$ , and  $c = 120 \text{ \AA}$ ,  $\beta = 110^\circ$ .

**Data collection and processing.** Data were collected at the Advanced Photon Source on Northeastern Collaborative Access Team beamline 24-ID-C on a Pilatus 6MF detector. Data were indexed and scaled in HKL2000(2). Resolution cutoffs were chosen as  $\text{CC1/2} \sim 0.8$ , which agrees with decrement of signal-to-noise ratio and  $R_{\text{sym}}$ . Data for the native crystal, the pyruvate soaked crystals and the CoA cocrystal extended to 2.60- $\text{\AA}$ , 3.00- $\text{\AA}$ , 3.20- $\text{\AA}$ , and 3.30- $\text{\AA}$  resolution, respectively.

**Structure determination and refinement.** The structure of native *Mt*PFOR was determined to 2.60- $\text{\AA}$  resolution by molecular replacement (MR) using Phaser(3) implemented in Phenix(4). The *Da*PFOR model (PDB ID: 2C42(5)), which shares more than 60% sequence identity with *Mt*PFOR, was trimmed with the Sculptor(6) algorithm implemented in Phenix(4) as the MR search model. The occupancy of TPP and [4Fe-4S] clusters were set to zero for MR search. The MR result gave a single solution of three copies of PFOR homodimer per asymmetric unit (ASU) with a log-likelihood gain (LLG) value of 18300 and a z-score of 114. One round of rigid-body refinement and simulated annealing was performed after MR, with initial  $R_{\text{work}}/R_{\text{free}} = 35\%/39\%$ . The atomic coordinates and B-factors were iteratively refined in Phenix Refine(4) with model building and manual adjustment of model in Coot(7). Water molecules were added manually throughout real space refinements using Fo-Fc electron density contoured to  $3.0\sigma$  as criteria. Non-crystallographic symmetry (NCS) restraints were used throughout refinement. Restraints for [4Fe-4S] clusters were based on *M. thermoacetica* carbon monoxide dehydrogenase/acetyl-CoA synthase (PDB ID: 3I01(8)). Restraints for TPP were based on the crystal structure of *Saccharomyces cerevisiae* pyruvate decarboxylase (PDB ID: 2VK8(9)). Final cycles of refinements include TLS parameterizations with three TLS groups per monomer, domain I-II, domain III, and domain IV-VI. The division of TLS groups is assigned to capture the flexible nature of domain III. The final model of the native structure contains residues listed in Table S2, one TPP per chain, and three [4Fe-4S]

clusters per chain.

Two structures of pyruvate-soaked *Mt*PFOR and one of *Mt*PFOR co-crystallized with CoA were determined to 3.00-Å, 3.20-Å, and 3.30-Å resolution by MR, respectively. The structure of native *Mt*PFOR was used as the MR search model in all cases. The MR results gave three dimers of PFOR per ASU in pyruvate-soaked *Mt*PFOR and three monomers of PFOR per ASU in CoA-cocrystallized *Mt*PFOR. In the latter case, two of the three monomers form a homodimer within the ASU, and the other monomer forms a homodimer with a monomer in a neighboring ASU across a crystallographic symmetry axis. The refinement protocol used was the same as for the native structure described above. However, additional restraints for CoA and the TPP adduct observed were required. In particular, restraints for CoA were based on the crystal structure of *Escherichia coli* acetyltransferase MccE (PDB ID: 3R9F(10)). Restraints for acetyl-TPP adduct and lactyl group of lactyl-TPP intermediate were generated from geometry optimizations followed by frequency calculations of 2-acetyl-3,4,5-trimethylthiazol-3-ium and 2-hydroxyl-2-methylpropanoate using B3LYP/6-311++G(11-13) with Gaussian 03(14). The calculated bond distances and angles for lactyl-TPP intermediate and acetyl-TPP adduct were used to update TPP restraints. The C2 of pyruvate in lactyl-TPP intermediate are restrained to be coplanar with the thiazolium ring. The carboxylic acid group and C2 of pyruvate in lactyl-TPP adduct are restrained to be planar. The acetyl group in acetyl-TPP adduct was restrained to be coplanar with the thiazolium ring. The final models contain three [4Fe-4S] clusters and one TPP or TPP adducts in each monomer. The model of PFOR cocrystallized with CoA contains one CoA molecule in each monomer. The detailed residue and TPP/TPP adduct composition is in Table S1 and S2.

Composite-omit electron density maps were calculated using Phenix(4) and used to verify all three models. All structure figures and solvent accessible surface area of proximal [4Fe-4S] clusters were rendered in PyMOL. Software used to process crystallography datasets was provided by SBGrid(15).

**Activity Assays with PFOR crystals.** Native PFOR crystals were grown to ~100x20x5  $\mu\text{m}^3$  as described above, washed sequentially in two 2- $\mu\text{L}$  of the crystallization well solution, and added to 2- $\mu\text{L}$  of assay solution. Assay solution consisted of 50 mM HEPES 8.0, 10 mM oxidized methyl viologen, and a combination of reagents as follows: Drop 1 of **Figure S6**– 5 mM pyruvate and 5 mM CoA (no crystal); Drop 2 – 5 mM CoA and

one crystal (no pyruvate), Drop 3 – 5 mM pyruvate and one crystal (no pyruvate); Drop 4 – 5 mM pyruvate, 5 mM CoA, and one crystal. Drops were sealed and reagents were allowed to incubate. Photos of drops were taken after 15 min and 12 hrs. After 12 hr, 1  $\mu$ L of 5 mM CoA was added to each drop and incubated for another 15 mins before the third photo was taken.

**Multisequence alignment.** Selection of representative sequences was described previously (16). Sequences of OORs, which do not bind CoA, were not included and sequences of *St*OFORs, which were not considered previously (16), were added. The alignment was performed using PROMAL3D(17). For sequences in which “domain III” is not the first domain of a protein chain, residues prior to domain III were manually removed before alignment to increase alignment quality. The full alignment is shown in Table S3. The UniProt IDs of sequences chosen and alignment results are shown in Table S4.

## SI Appendix – Figures

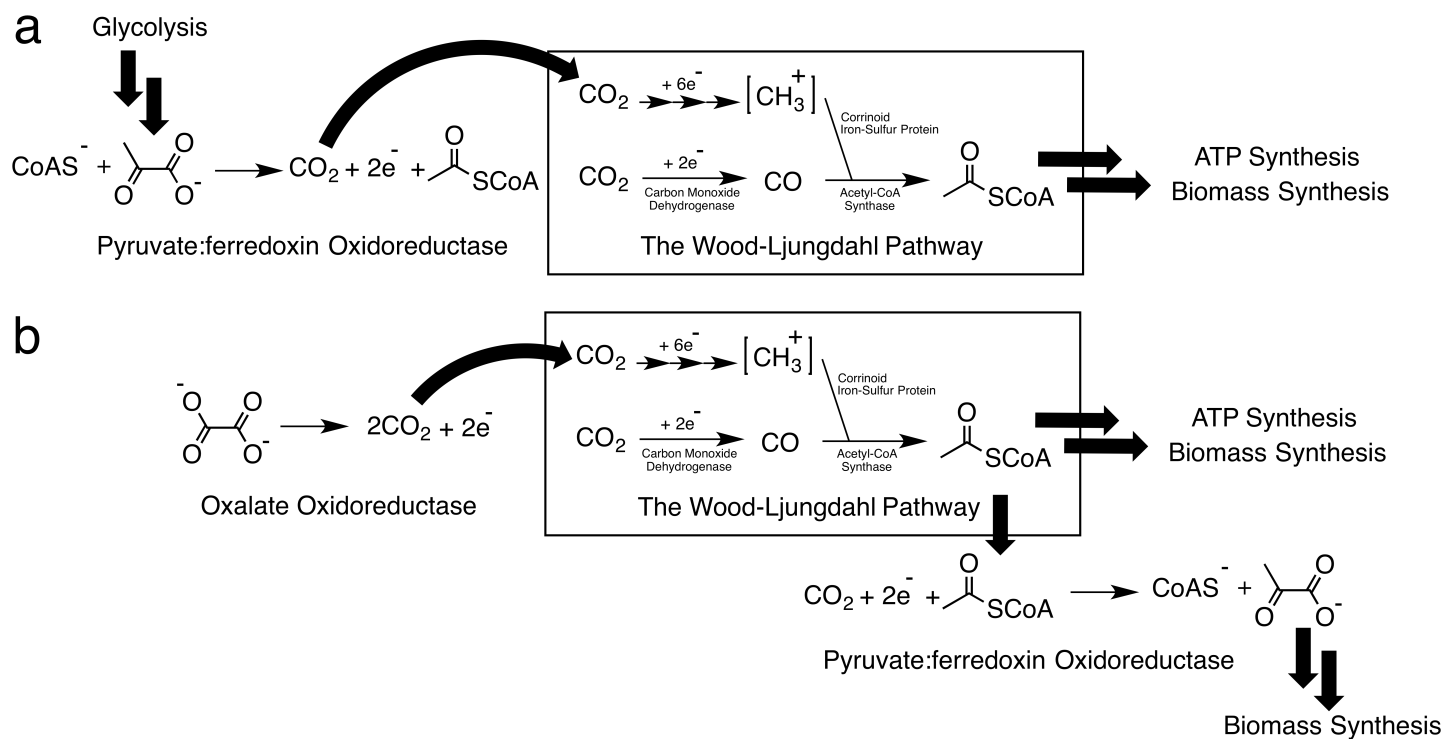


**Figure S1. Relationships of PFOR and OOR to the Wood-Ljungdahl pathway.** (a) Pyruvate from glycolysis is cleaved by PFOR, and the products can feed into the Wood-Ljungdahl pathway under certain cellular conditions. (b) OOR cleaves oxalate, generating both carbon dioxide and electrons for the Wood-Ljungdahl pathway. PFOR can convert the acetyl-CoA that is produced by the Wood-Ljungdahl pathway into pyruvate.

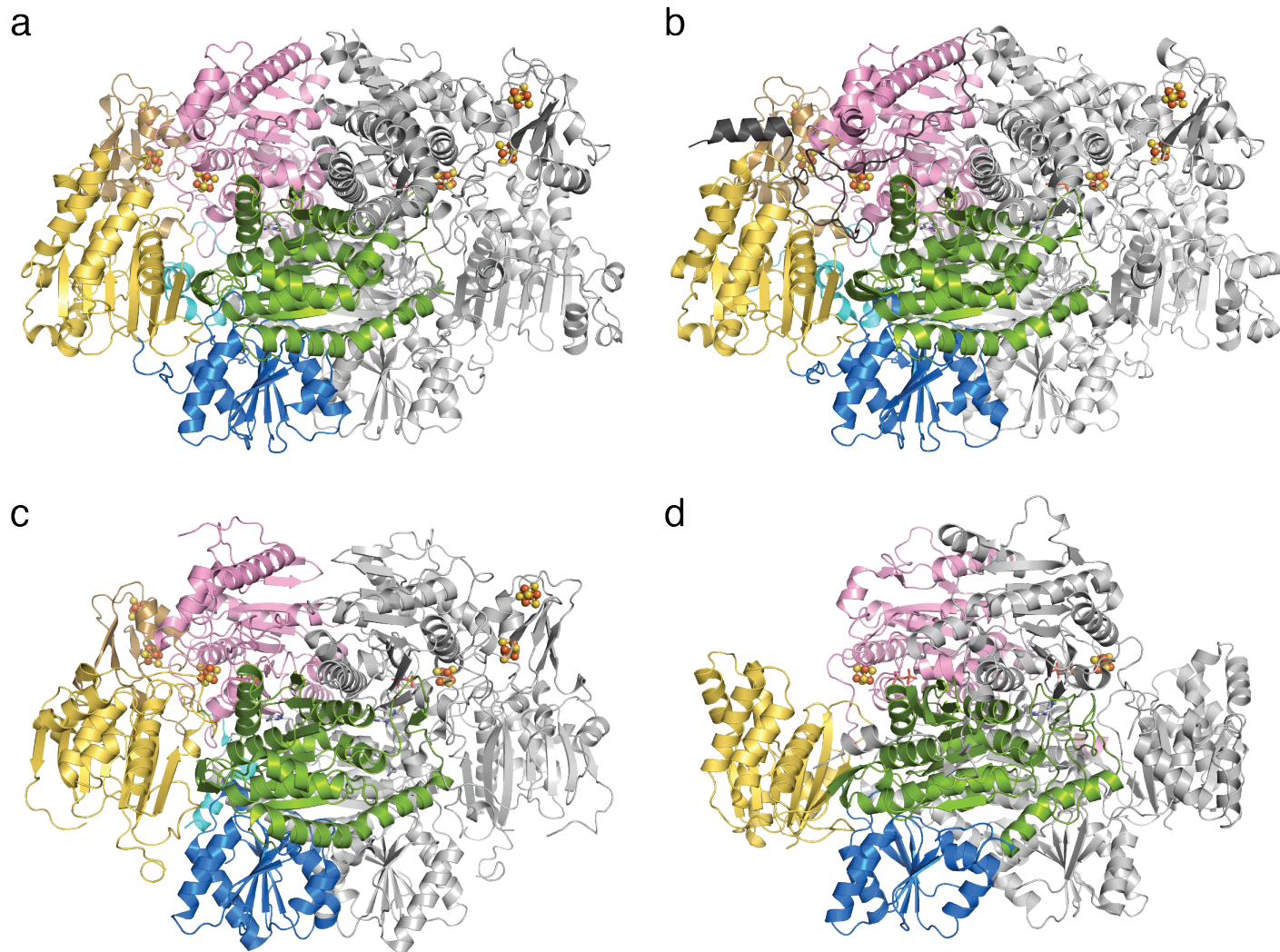


**Figure S2. Overall OFOR structures.** (a) *MtPFOR* (b) *DaPFOR* (PDB ID: 2C3M(5)) (c) *MtOOR* (PDB ID: 5C4I(18)) (d) *StOFOR2* (PDB ID: 5B46(19)) Both *MtPFOR* and *DaPFOR* are  $\alpha_2$  homodimers and are very similar in terms of overall structure. One difference is that domain VII is only found in OFORs from the *Desulfovibrio* genus. *MtOOR* is a  $(\alpha\beta)_2$  dimer of heterotrimers. Both structurally characterized *StOFORs* are dimers of heterodimers  $(\alpha\beta)_2$  in which chain  $\alpha$  contains domains I, II, and III, but the order of the domains with respect to the primary sequence is domain III-I-II from N-terminus to C-terminus. Color schemes and domain arrangements are in **Figure 2A**; domain VII of DaPFOR is shown as black ribbons.

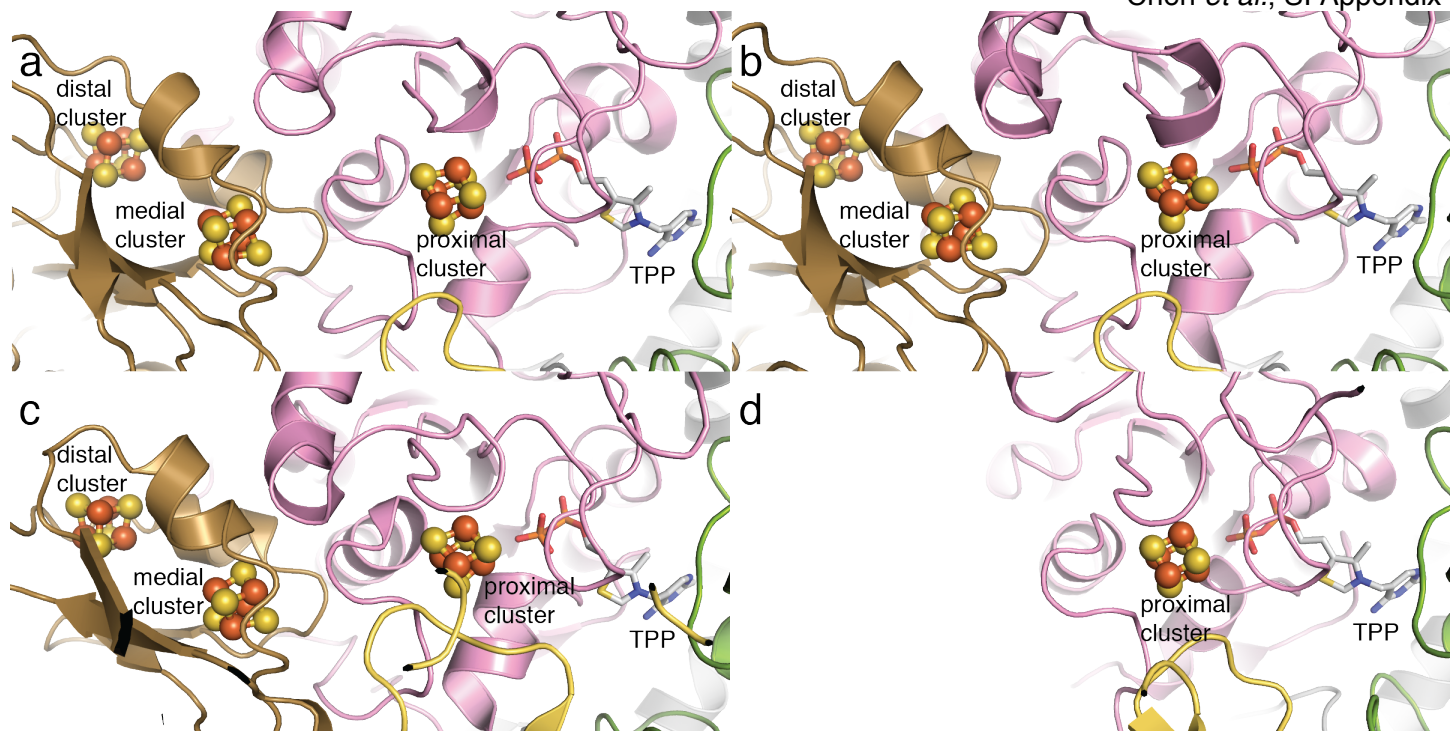


**Figure S3. The redox active cofactors are oriented similarly.** (a) *MtPFOR* (b) *DaPFOR* (PDB ID: 2C3M(5)) (c) *MtOOR* (PDB ID: 5C4I(18)) (d) *StOFOR2* (PDB ID: 5B46(19)). Despite the differences in functions and oligomeric states, each catalytic unit adapts a similar fold that binds one [4Fe-4S] cluster and one TPP through domain VI and two [4Fe-4S] clusters in domain V. *StOFOR2s* lack domain V, but TPP and the only enzyme-bound [4Fe-4S] cluster are arranged in a similar orientation with respect to the other OFORs. TPP molecules are drawn in sticks. [4Fe-4S] clusters are drawn in ball-and-stick representations. Domain I, III, V and VI of each protein) are shown as ribbons in the same color scheme as **Figure 2a**.

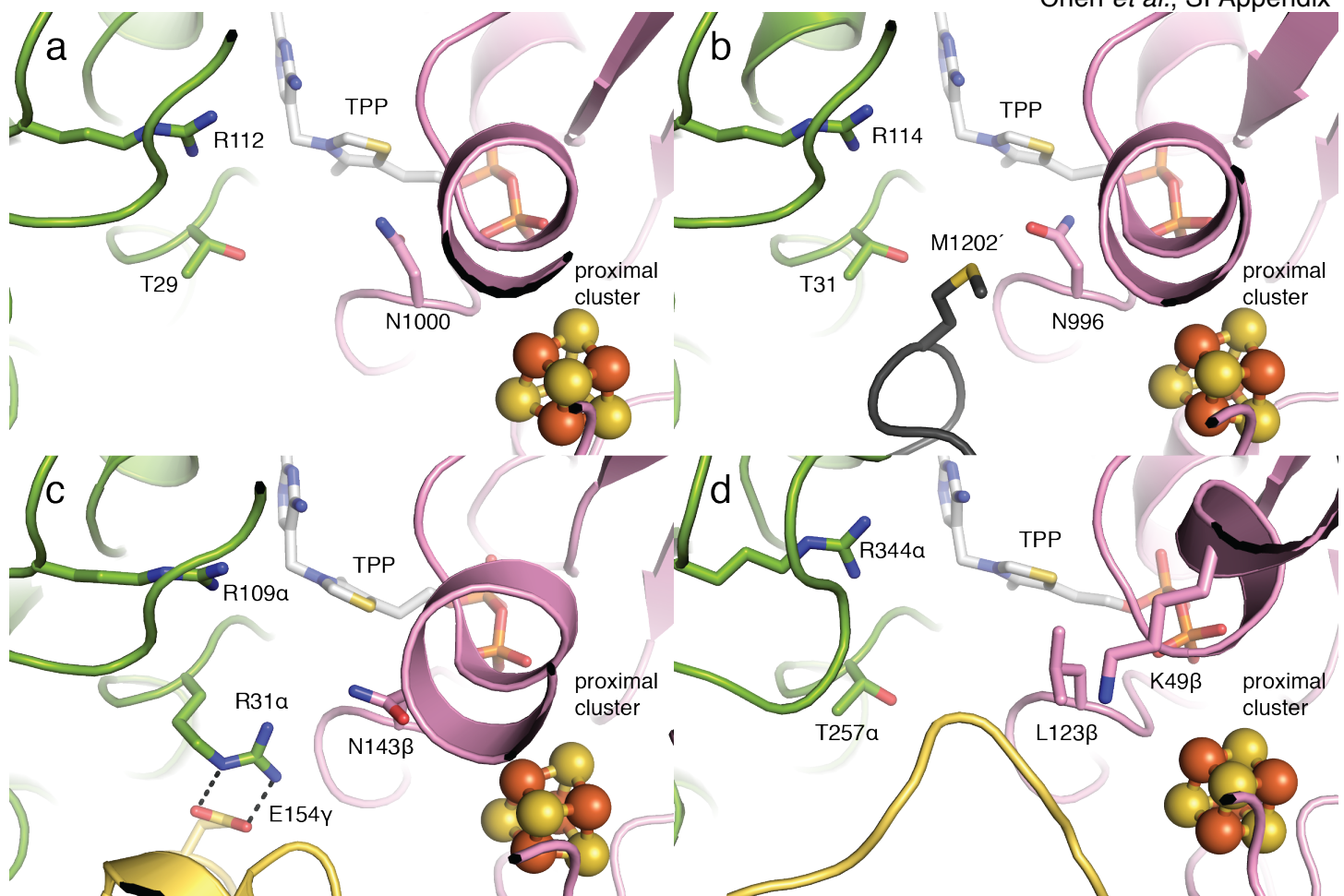


**Figure S4. Active site residues in OFOR enzymes.** (a) *MtPFOR* (b) *DaPFOR* (PDB ID: 2C3M(5)) (c) *MtOOR* (PDB ID: 5C4I(18)) (d) *StOFOR2* (PDB ID: 5B46(19)). The active site residues are conserved between *MtPFOR* and *DaPFOR* except for Met1202', which belongs to *DaPFOR*'s domain VII. Met1202' plugs the active site, and thus pyruvate-binding residues are not solvent accessible in the crystal structure of *DaPFOR*. Active site residues in *MtOOR* are similar to what is found in PFORs except Arg31α replaces Thr29 (*MtPFOR* numbering). The difference affords a more electrostatic positive active site to bind oxalate, a dicarboxylic acid. The active site of *StOFOR* is larger than the other structurally characterized OFORs and contains two positively charged residues, Arg334α and Lys49β. The figures are in the same orientation as **Figure 4E**. Domain I, III and VI of each protein are shown as ribbons in the same color scheme as **Figure 2A**; domain VII of *DaPFOR* is shown as black ribbons. Active site residues and TPP molecules are drawn in sticks. [4Fe-4S] clusters are drawn in ball-and-stick representations.

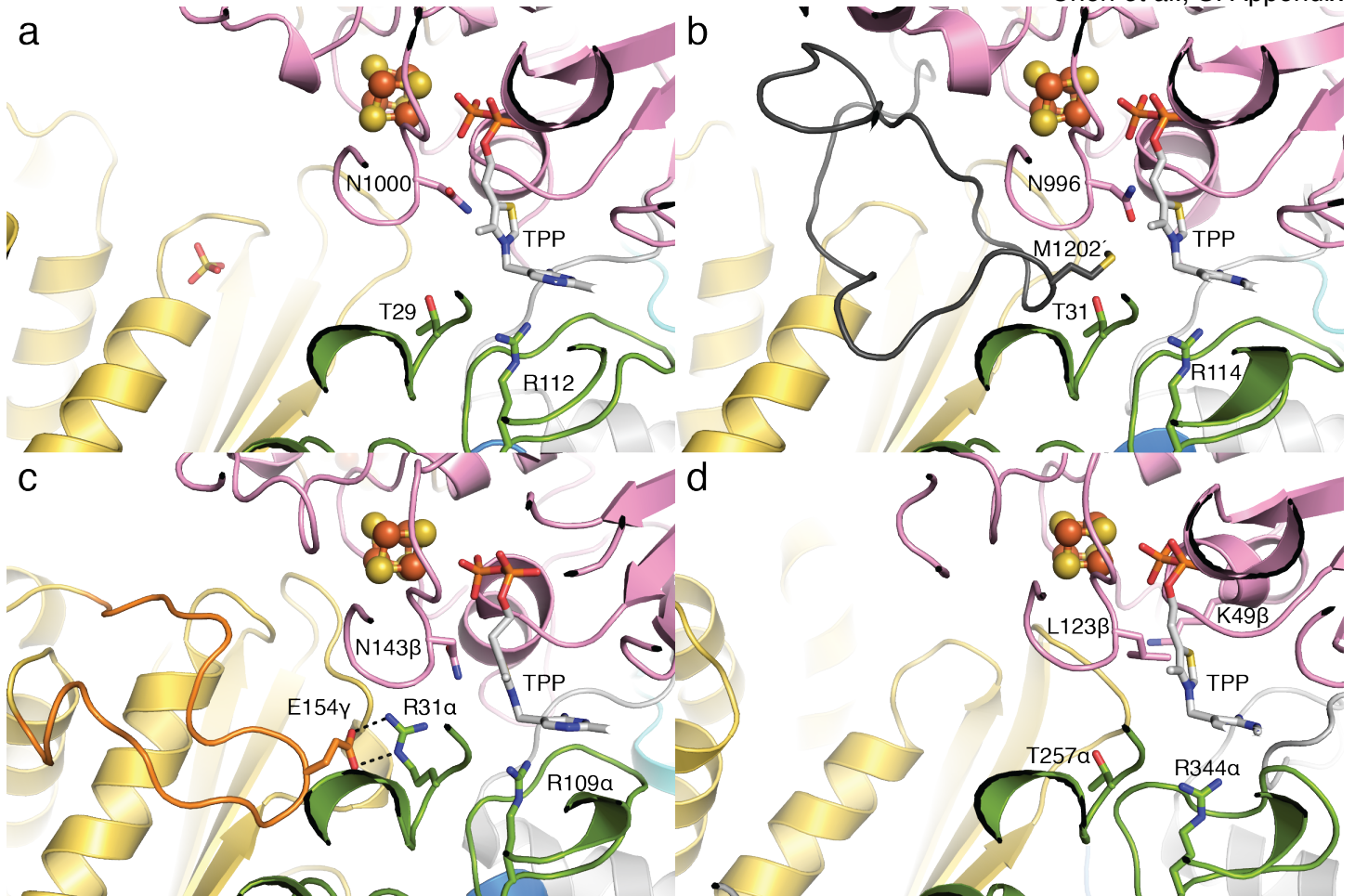


**Figure S5. Differences in active site accessibility in OFORs.** (a) The active site of *MtPFOR* is open. Thr29 and Asn1000, which were identified as pyruvate-binding residues are solvent accessible. (b) The active site of *DaPFOR* (PDB ID: 2C3M(5)) is blocked by domain VII (black) from the other monomeric subunit of the homodimer in the crystal structure. (c) The active site of *MfOOR* in the resting state (PDB ID: 5C4I(18)) is blocked by an extension from domain III referred to as the plug loop (orange). (d) The active site of *StOFOR2* (PDB ID: 5B46(19)) is open. The figures are in the same orientation as **Figure 4A**. Domain I, III and VI of each protein are shown as ribbons in the same color scheme as **Figure 2A**. Active site residues and TPP molecules are drawn in sticks. [4Fe-4S] clusters are drawn in ball-and-stick representations.

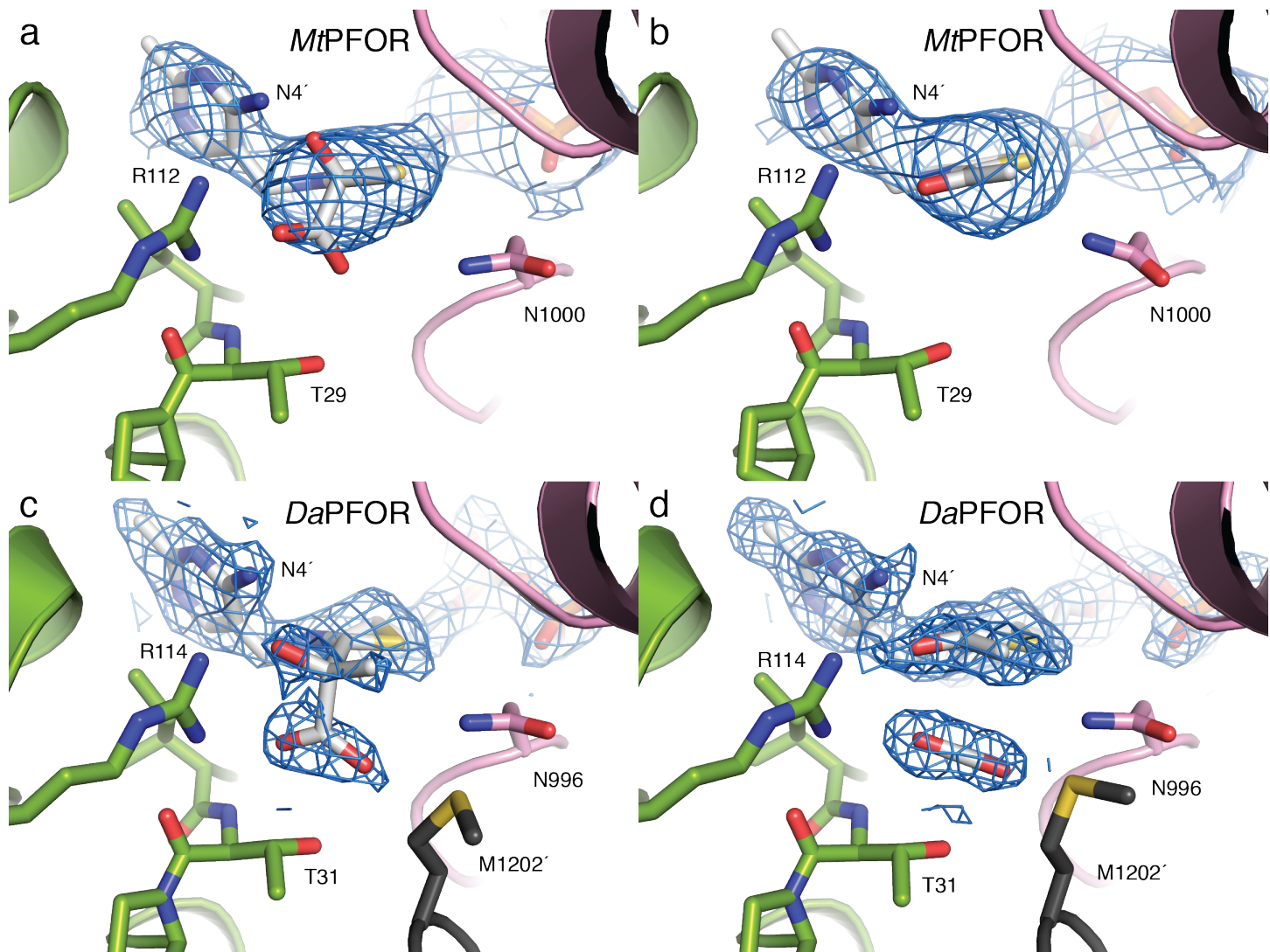


**Figure S6. The electron density of lactyl-TPP intermediates and acetyl-TPP adduct observed in *MtPFOR* and *DaPFOR*.** (a) Composite-omit electron density map contoured to  $1.0 \sigma$  in blue mesh for *MtPFOR* soaked with pyruvate for 15-min. Lactyl-TPP intermediate state is modeled in the electron density. Four of six active sites in the asymmetric unit (ASU) show omit map density indicative of adduct formation. (b) Composite-omit electron density map contoured to  $1.0 \sigma$  in blue mesh for *MtPFOR* soaked with pyruvate for 12-hr. An acetyl-TPP adduct is modeled in the electron density. Density for an acetyl-TPP adduct is present in all six active sites in ASU. (c) 2Fo-Fc electron density map contoured to  $1.0 \sigma$  is shown for lactyl-TPP intermediate state in *DaPFOR* (PDB ID: 2C3P(5)). The carbon-carbon bond between C2 carbon of TPP and the lactyl moiety is long at 1.9-Å. (d) 2Fo-Fc electron density map contoured to  $1.0 \sigma$  for acetyl-TPP intermediate in *DaPFOR* (PDB ID: 2C3Y(5)). Carbon dioxide are refined into density near the acetyl-TPP adduct.



**Figure S7. Crystallized PFOR retains pyruvate oxidation activity.** Each 2-  $\mu\text{L}$  drop contains 50 mM HEPES pH 8.0, 10 mM oxidized methylviologen (MV) and a combination of substrates as follows: Drop 1 – negative control drop (no crystal) containing 5 mM CoA and 5 mM pyruvate; Drop 2 – negative control drop (no pyruvate) containing one crystal and 5 mM CoA; Drop 3 – negative control drop (no CoA) containing one crystal and 5 mM pyruvate; Drop 4 – one crystal, 5 mM CoA and 5 mM pyruvate. Crystals were looped and washed, before being added into each drop. (a) Results of 15 min incubation. MV is reduced in drop 4 turning the solution purple, but not in the negative control drops (1-3) (b) Results of 12 hr incubation. No MV reduction is observed in control drops (1-3). (c) Following a 12 hr incubation, 1  $\mu\text{L}$  of 5 mM CoA was added into each drop and allowed to incubate for 15 min. With the addition of CoA to all drops, Drop 3 (the no CoA control) now turns purple.

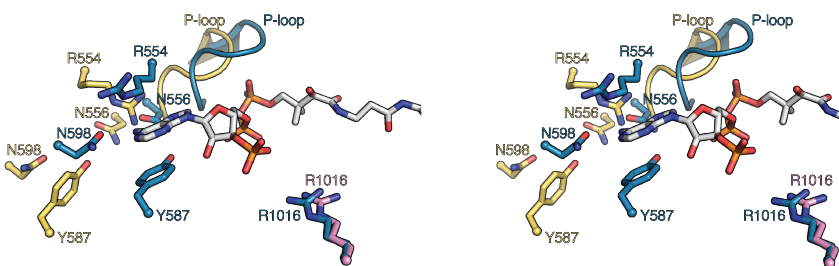


**Figure S8. Stereo view showing that residues that contact CoA are not pre-organized for CoA binding.** Adenine binding residues (sticks) and P-loop (ribbons) adopt different conformations with CoA (teal) and without (yellow). Movement of domain III also brings 3'-phospho group of CoA toward Arg1016 (without CoA – pink; with CoA – teal). Cas are labeled as spheres.

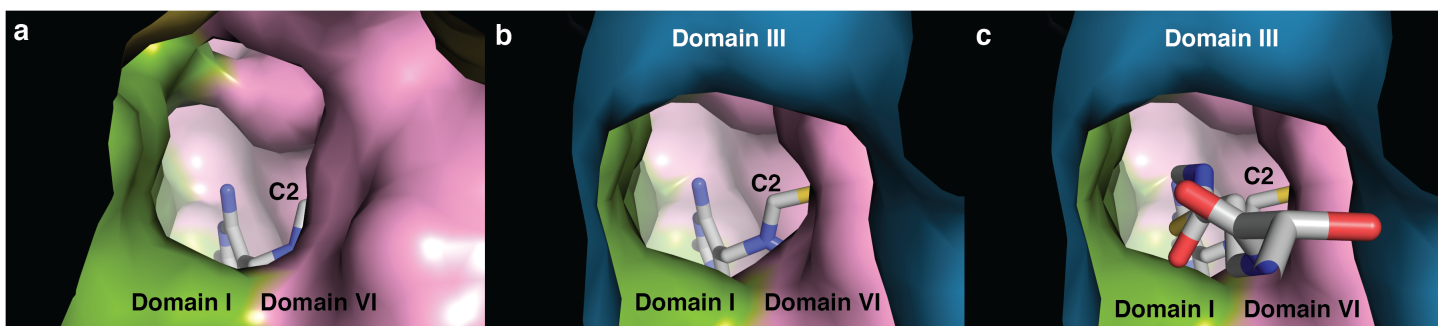


**Figure S9. Surface representations of the MtPFOR active site in different liganded states.** (a) Channel to TPP is open in the CoA-free structure of MtPFOR. (b) Channel to TPP is narrower in the CoA-bound structure of MtPFOR due to movement of domain III (teal surface). CoA is omitted for clarity. (c) CoA-bound MtPFOR structure showing CoA filling the narrow channel to TPP, occluding the TPP from solvent. CoA and TPP are shown as sticks. Position C2 of TPP, which initiates the nucleophilic attack on pyruvate, is labeled. Domain I surface is in green, domain III in teal, and domain VI in pink.

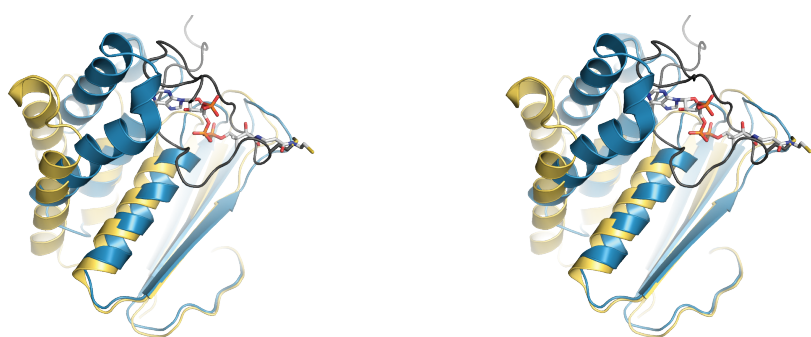


**Figure S10. Stereo view of domain III and VII of DaPFOR (PDB ID: 2C3M(5)) overlaid with domain III of MtPFOR from CoA-bound structure.** Domain VII of DaPFOR (black) occupies the space where CoA binds in MtPFOR and clashes with CoA-bound position of MtPFOR's domain III. Domain III of MtPFOR with CoA bound is colored teal; domain III of DaPFOR is colored yellow.

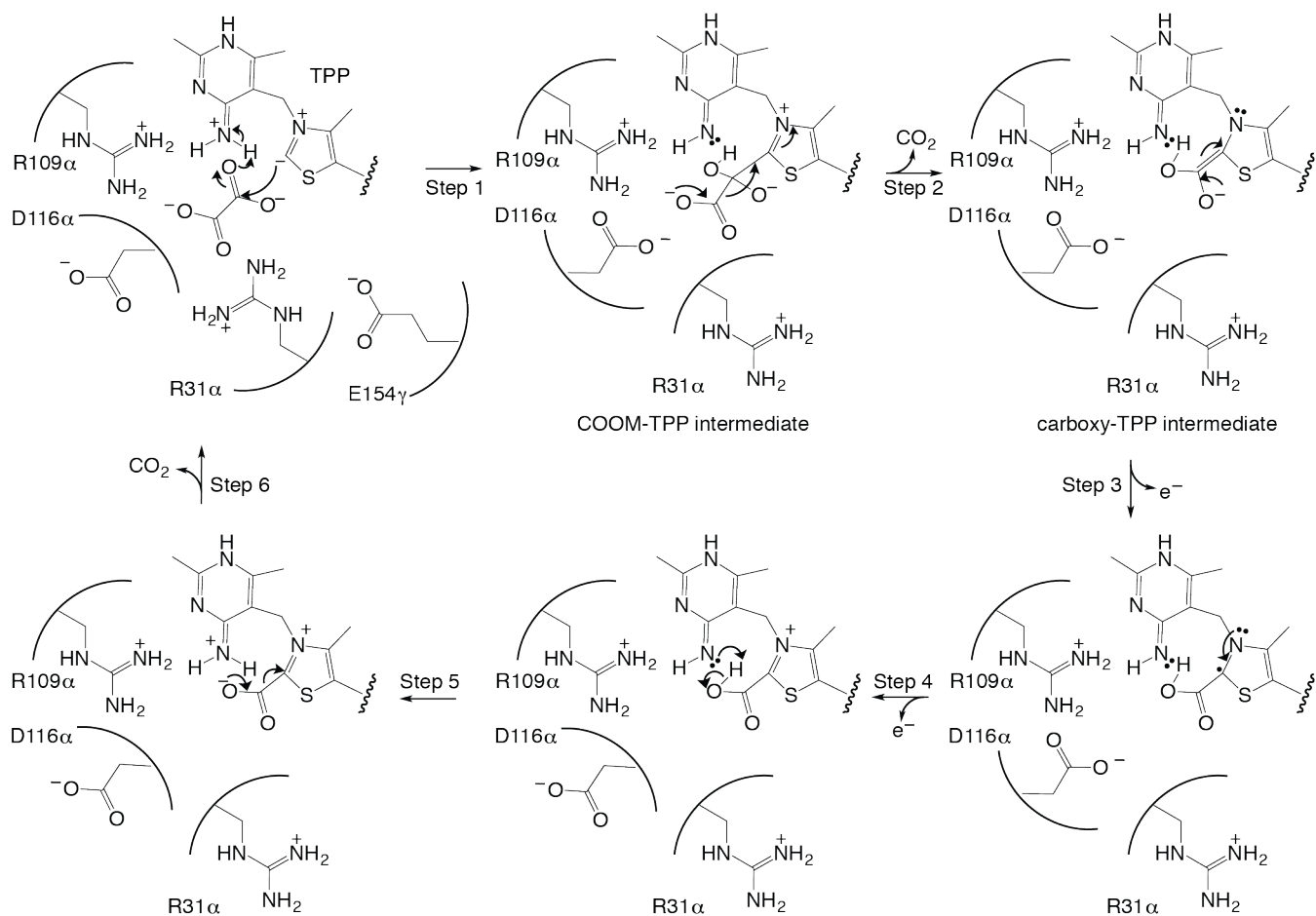


**Figure S11. A bait-and-switch mechanism proposed for OOR.** This mechanism for *MtOOR* has been proposed based on structural snapshots of *MtOOR*(18, 20) and computational studies of reaction intermediates (21-24). Active site residues Arg31 $\alpha$  and Arg109 $\alpha$  are proposed to activate oxalate, a dicarboxylic acid, for nucleophilic attack by the TPP, and protonation of the carboxy-di-oxido-methyl-TPP (COOM-TPP) is proposed to occur with the N4' of TPP acting as the catalytic acid (**step 1**). Asp116 $\alpha$ , which is part of a loop called the ‘switch loop’, is observed by crystallography to flip into the active site and point directly toward the COOM-TPP adduct, which is expected to facilitate decarboxylation through charge-charge repulsion (**step 2**). CO<sub>2</sub> release further requires movement of Arg31 $\alpha$  out of the active site, which additionally alters the active site electrostatic environment to be less positively charged. Arg31 $\alpha$  is not free to move, however, without the accompanying movement of domain III and the so-called plug loop that houses Glu154 $\gamma$ . The plug loop is named for the fact that it ‘plugs’ the active site burying the COOM-TPP adduct. The ‘plugging’ is secured by interaction between Glu154 $\gamma$  and Arg31 $\alpha$ . Following decarboxylation, the first electron is transferred to a [4Fe-4S] cluster (**step 3**) and then the second electron is transferred (**step 4**). It has been proposed that the presence of negatively charged Asp116 $\alpha$  in the active site facilitates these oxidations through charge repulsion (20). In the last step before release of the second CO<sub>2</sub> (**step 5**), Asp116 $\alpha$  has been proposed to flip back, away from the active site, consistent with one crystal structure of a carboxyl-TPP intermediate in *MtOOR*. This loop rearrangement removes the negative charge next to the carboxyl-TPP, thus facilitating deprotonation of the carboxylate and CO<sub>2</sub> release (**step 6**).

**SI Appendix – Tables****Table S1. Data collection and model refinement statistics of MtPFOR**

PDB ID	Native 6CIN	Pyruvate soaked (15 mins) 6CIO	Pyruvate soaked (12 hrs) 6CIP	CoA cocrystallization (10 mM) 6CIQ
Beamline	APS 24-ID-C	APS 24-ID-C	APS 24-ID-C	APS 24-ID-C
Space group	C2	C2	C2	C2
Cell dimensions (Å)	a=340.61, b=106.63, c=239.08, β=109.31°	a=340.39, b=107.10, c=239.56, β=109.67°	a=342.01, b=108.26, c=240.44, β=109.32°	a=337.71, b=106.99, c=120.47, β=109.85°
Wavelength (Å)	0.9791	0.9791	0.9789	0.9789
Resolution (Å)	100.-2.60 (2.64-2.60)	50.-3.00 (3.11-3.00)	100.-3.20 (3.26-3.20)	100.-3.30 (3.36-3.30)
# unique reflections	247841	157684	133390	58817
Completeness (%)	98.5 (95.7)	97.4 (92.6)	97.1 (84.9)	97.3 (83.0)
Redundancy	3.3 (3.0)	4.9 (4.1)	3.3 (2.7)	3.5 (2.7)
<l/σl>	9.4 (2.1)	7.2 (1.7)	7.4 (1.5)	6.1 (2.1)
R <sub>sym</sub>	0.075 (0.582)	0.160 (0.793)	0.092 (0.580)	0.159 (0.454)
CC <sub>1/2</sub>	(0.796)	(0.781)	(0.836)	(0.798)
Resolution (Å)	89.0 - 2.60	48.5 - 3.00	97.5. - 3.20	80.3 - 3.30
# unique reflections	244551	157125	132694	58800
R <sub>work</sub> (%) / R <sub>free</sub> (%)	19.5/22.7	20.7/24.1	18.7/22.5	18.4/22.3
RMS bond lengths (Å)	0.003	0.003	0.003	0.003
RMS bond angles (°)	0.561	0.554	0.550	0.566
Number of Atoms/Molecules				
Protein atoms	53090	53163	52606	26589
TPP	6	2	0	3
Lactyl-TPP	0	4	0	0
Acetyl-TPP	0	0	6	0
[4Fe-4S] clusters	18	18	18	9
CoA molecules	0	0	0	3
Water molecules	439	54	27	29
Average B-factor (Å <sup>2</sup> )	77.5	75.3	103.4	95.0
Protein chains	77.7	75.5	103.5	95.0
TPP	68.9	69.0	n/a	66.7
Lactyl-TPP	n/a	61.1	n/a	n/a
Acetyl-TPP	n/a	n/a	89.9	n/a
[4Fe-4S] clusters	88.4	86.5	112.1	95.3
CoA molecules	n/a	n/a	n/a	127.1
Water molecules	51.3	36.5	57.1	40.1
Ramachandran plot				
Favored (%)	98.45	98.40	98.31	97.93
Allowed (%)	1.55	1.60	1.69	2.07
Outliers (%)	0.00	0.00	0.00	0.00
Rotamer outliers (%)	0.37	0.42	0.41	0.40

**Table S2. Residues and cofactors modeled in each chain of all four structures.**

	Chain					
	A	B	C	D	E	F
Native	2-1140, 1147-1170, 3 [4Fe-4S], 1 TPP	2-1170, 3 [4Fe-4S], 1 TPP	2-623, 630-1170, 3 [4Fe-4S], 1 TPP	3-586, 592-622, 629-1170, 3 [4Fe-4S], 1 TPP	2-625, 630-1170, 3 [4Fe-4S], 1 TPP	3-586, 597-1170, 3 [4Fe-4S], 1 TPP
Pyruvate soaking (15 mins)	2-1140, 1146-1170, 3 [4Fe-4S], 1 lactyl-TPP	2-1140, 1146-1170, 3 [4Fe-4S], 1 TPP	2-623, 632-1170, 3 [4Fe-4S], 1 lactyl-TPP	2-587, 594-624, 629-1170, 3 [4Fe-4S], 1 lactyl-TPP	2-622, 632-1142, 1146-1170, 3 [4Fe-4S], 1 TPP	2-587, 594-622, 631-1170, 3 [4Fe-4S], 1 lactyl-TPP
Pyruvate soaking (12 hrs)	2-1140, 1145-1170, 3 [4Fe-4S], 1 acetyl-TPP	2-1140, 1145-1170, 3 [4Fe-4S], 1 acetyl-TPP	2-623, 630-1170, 3 [4Fe-4S], 1 acetyl-TPP	2-624, 630-1170, 3 [4Fe-4S], 1 acetyl-TPP	2-624, 630-1170, 3 [4Fe-4S], 1 acetyl-TPP	2-1170, 3 [4Fe-4S], 1 acetyl-TPP
CoA cocrystallization	2-1170, 3 [4Fe-4S], 1 TPP, 1 CoA	2-624, 628-1170, 3 [4Fe-4S], 1 TPP, 1 CoA	2-622, 631-1170, 3 [4Fe-4S], 1 TPP, 1 CoA	N/A	N/A	N/A

**Table S3. Sequence alignments of domain IIIIs of CoA-dependent OFORs.** The sequences are arranged in the same order as Table S4.

Conservation:		8 66 9	
sp_005650_PORC_THEME_Pyru	1	-----MPVAKKYFEIRWHGRAGQGAKSASQMLAEAA-LEAGKYVQAFPEYGAER	48
tr_M3NSB1_M3NSB1_HELPX_Py	1	-----MFQIRWHARAGQQAITGAKGLADVI-SKTGKEVQAFASYGSAK	42
tr_Q3Z8I7_Q3Z8I7_DEHM1_Py	1	-----MKHFIEIRWHGRGGQQAVTSALIAQAA-IGKGKYAQAFPSFGPER	45
sp_P80523_PORC_METBF_Pyru	1	-----MKEIRIHGRGGQQSVTAEMLSVAAC-FEDGKFSQAFPAFGVER	42
sp_P80902_PORC_METTM_Pyru	1	-----MIEIRFHGRGGQQAVTAEILAKAA-FEDGKYSQAFPFFGVER	42
tr_W8CQB1_W8CQB1_9EURY_Py	1	-----MIEIRFHGRGGQQAVTAANILAEAA-FLEGKYVQAFPFFGVER	42
tr_Q4KY23_Q4KY23_TRIVA_Py	411	-----PEGTKQCMFWGLGSDCTVGANKQAIKLIVSNTKLYGQAYFAYDAHK	456
sp_P94692_POR_desaf_Pyruv	414	-----PKGTIQCFWGLGADCTVGANKQAIKIIGDNTDLFAQGYFSYDSKK	459
tr_Q2RMD6_Q2RMD6_MOOTA_Py	411	-----PKGTFRKCFWGLGSDCTVGANKNSKIIIGDHTDMYAQGYFVYDSKK	456
tr_C4LTX6_C4LTX6_ENTHI_Py	409	-----PEGTTQCMFWGLGSDCTVGANHDAIRIIGQNTDMYVQGYFSYDAHK	454
sp_Q968X7_PNO_CRYPV_Pyruv	417	-----TSETKQCLFWGLGSDCTVSANKNAIKIIGESTDLQVQGYFAYDAKK	462
sp_Q941N5_PNO_EUGGR_Pyruv	480	-----PEGTRQCVFWGIGSDCTVGANRSAVRIIGDNSDLMVQAYFQFDAFK	525
tr_L8B958_L8B958_CHLRE_Py	522	-----PKGTFECLFWGMGSDCTVGANKKEAIKIIASSAGMSAQAYFSYDAHK	567
sp_Q53046_NIFJ_RHORT_Pyru	422	-----SADIKRSPWGLGADCTVGANKNSKIIISDSPTIHGQGYFVYDSKK	467
tr_B5XPH3_B5XPH3_KLEP3_Py	414	-----HAGITACKFWGMGSDCTVGANKSAIKIIGDNTPLYAQAYFSYDSKK	459
tr_Q24982_Q24982_GIAIN_Py	437	-----PEGTTECILWGLGSDCTIGACRANAKILSDRVCCECQANFEFDGKK	482
tr_I2K9Y6_I2K9Y6_9PROT_Py	1	-----MAEQKKKERYNIRISGLGGQQGVTTAHLGSTM-DNAGKYASLVPFFGSEK	50
tr_O67231_O67231_AQUAE_Fe	1	-----M-KRYNIRIAVGGGQGVVTSAAHIIIGNAM-AAAGKYASLVPFFGSEK	44
tr_I0IRW0_I0IRW0_LEPFC_Fe	1	-----MNKERNIRMAIGGGQGVVTASHILSNGM-VIMGGESTLVPFFGSEK	46
tr_J9ZD37_J9ZD37_LEPFM_Py	1	-----MSAMKRRNIRMGLGGQQGVVTSAAHIMAMA-SKEDKFSISNPFFGAEK	48
tr_D3DJJ8_D3DJJ8_HYDTT_Py	1	-----MKRRRNIRMAPALGGQQAVTAHHIATAA-DYEYYAVSNPNFFGAEK	46
sp_P84820_PORC_THELN_Pyru	1	-----MIEIRFHGRGGQQAVTAANILAEAA-FLEGKYVQAFPFFGVER	42
sp_P80907_VORA_METTM_Keto	290	-----DDPEFREVVKIAFGGGQQVLSMGLTLAQAA-CSEGRHTSWYPAYGPEQ	337
tr_A1HTT9_A1HTT9_9FIRM_Py	1	-----MTHEIIIMAGFGGGQGVMLMGQLVTYAG-MIEGKQVSWIPSYGPEM	43
tr_B0R3G0_B0R3G0_HALS3_Ox	1	-----MHDDLNAIWIGGEAGDGIASTGKIFQAAL-SRAGRHVFTSKDFASRI	45
tr_H3ZPH3_H3ZPH3_THELN_2-	1	-----MQIRLAGIGGGQGVVLAGIILGEAA-AIEGLNVIQTDYGSQS	41
tr_Q1IOP1_Q1IOP1_KORV_2-	1	-----MQRLQLTETIRIAFGGGQQGVILSAIVIGKAASILEGGFATMTOQSGFPEA	48
tr_E8RJ92_E8RJ92_DESPD_2-	1	-----MSKNAPSSQTEIIVTGFGGGQGIIILAGRILGMAASLGDKESTLVOAYGPES	51
sp_P80906_KORC_METTM_2-ox	1	-----MRKEIRIAFGGGQGVILAGIVLGAASLYDGLYAVQTOQSYGPEA	44
tr_O68230_O68230_HELPX_Oo	1	-----MEAQLRFTGVGGQGVLLAGEIILAEAK-IASGGYGTKTSTYTSQV	43
sp_053182_KORA_MYCTU_2-ox	1	-----MDPNNGAGPESHDAAFHAAPDRQRLENVIRFAGDSGDQMQLTGDRTSEA-ALFGNDLATQPNTYPAEI	69
tr_H0DIR4_H0DIR4_9STAP_2-	1	-----MRNQISWKVGQQGEGIESTGEIFATAM-NRKGYLYGYRHFSSRI	45
tr_087870_087870_THAAR_2-	1	-----MTARSVISITFAGSGGGAGVMTAGSMILDAA-GHAGWYAYMTRSSGAQI	46
tr_B0R4X6_B0R4X6_HALS3_Py	1	-----MTDDELIWRIAGGSGDIDSTSQNFAKAL-MRSGLDVFTHRHPSRI	46
tr_D3DI99_D3DI99_HYDTT_2-	1	-----MAFDLTIKIGGEGEGEVISAGDFLTESA-ARAGYYVNFKSPFAEI	45
sp_007836_IORB_THEKO_Indo	1	-----MKEYNIVITGVGGQGILTAANLLGWAA-LRAGYKVRVGEVHGMSQ	44
tr_A1RYA4_A1RYA4_THEPD_In	1	-----MAGKSIVIAVGGGQQLITIGTVVAQL-IRKGYSVRGEVHGMSQ	44
tr_K4MBD5_K4MBD5_9EURY_In	1	-----MSAPGISQFDVIIAGVGGQGAILASDIIGKAA-VKENLSVRAAETHGMAQ	49
sp_P80911_IORB_METTM_Indo	1	-----MSNYIYVGVGGQQIICKTSVIIGEAA-MNEGMMVVMSIEHGMAQ	43
tr_P72578_P72578_SULSP_2-	1	-----MRLSWVIGGAQGTCIDTAANIFGNNAV-ASAGYYIYGNREYYSNI	43
tr_Q96Y66_Q96Y66_SULTO_2-	1	-----MRLSWVIGGAQGTCIDTAANIFGNNAV-ASAGYYIYGNREYYSNI	43
tr_Q96XT2_Q96XT2_SULTO_2-	1	-----MTRIVWMIGGAQGLGVDTSANIFGNNAV-AKAGYYLFGNRREYYSNI	44
<u>Consensus_aa:</u>		.....ph.h.G.ttpGh...hsp.h.phh....s....@ssp.	

Yellow – P-loop

Red – Positively charged residue predicted to be within hydrogen bond distance with the proximal [4Fe-4S] cluster

## Conservation:

	6	6	6	
sp_005650_PORC_THEME_Pyru	49	TG-----APMRAFNIRGDEYIRVRS-AVENPDVVVVVIDETLLSP-----	AIVEGLSED	95
tr_M3NSB1_M3NSB1_HELPX_Py	43	RG-----AAMMAYNRVDEEPILNHE-RFMQPDYVLVIDPGLVFIE-----	NIFANEKED	90
tr_Q3Z8I7_Q3Z8I7_DEHM1_Py	46	RG-----APVQSFNRISDDKPIRERSGISEPDIIVVVLDPSLVIIG-----	NVISGLKEG	94
sp_P80523_PORC_METBF_Pyru	43	RG-----APVQAFTRINNNPIRLRS-QVYTPDYVIVQDATLLETV-----	DVASGVKDD	90
sp_P80902_PORC_METTM_Pyru	43	RG-----APVMAFTRINDEPIRRRY-QVYNPDYVVVLDEGLVDVV-----	DVFSGLKED	90
tr_W8CQB1_W8CQB1_9EURY_Py	43	RG-----APVTAFTRIDEKPIRIKT-QIYEPDIVVVLDPSSLDTV-----	DVTAGLKDG	90
tr_Q4KY23_Q4KY23_TRIVA_Py	457	SG-----GVTPPHLRGAKPINAPY-QVQNADYIACHNPSYLHKF-----	DMTKQLKKG	504
sp_P94692_POR_DESAF_Pyruv	460	SG-----GITISHLRFGEKPIQSTY-LVNRADYVACHNPAYVGTY-----	DILEGIKDG	507
tr_Q2RMD6_Q2RMD6_MOOTA_Py	457	SG-----GVTISHLRFQKQPIQSAY-LIDQADLIACHNPSYVGRY-----	NLLEGIKPG	504
tr_C4LTX6_C4LTX6_ENTHI_Py	455	SG-----GVTVSHLRFQKQPIKSQY-LIQNADYTACHFPNVKKY-----	KLLDAAKPN	502
sp_Q968X7_PNO_CRYPV_Pyruv	463	AG-----GATMSHLRFGPKPQKPSAY-LLQRCDYVAVHHPSYVHKF-----	DVLENIKQG	510
sp_Q941N5_PNO_EUGGR_Pyruv	526	SG-----GVTSSHRLRFGPKPITAQY-LVTNAODYIACHFQEYVKRF-----	DMLDAIREG	573
tr_L8B958_L8B958_CHLRE_Py	568	SG-----GVTVSHLRFGPSPIDSPY-LVQOQDYLAVNHQSYMAYK-----	DTLASLPKG	615
sp_Q53046_NIFJ_RHORT_Pyru	468	SG-----AITISHLRFGPPIRAPY-LIDEADFIACHHFSFLDKV-----	DVLETAAVG	515
tr_B5XPH3_B5XPH3_KLEP3_Py	460	SG-----GITVSHLRFGDRPITSPTY-LIHRADFIACSQQSYVDRY-----	DLLEGLPKG	507
tr_Q24982_Q24982_GIAIN_Py	483	SG-----GTTVSHLRFGPKKIRAQY-NIEEAGYVACHAQSYVSFK-----	NVLHGIKED	530
tr_I2K9Y6_I2K9Y6_9PROT_Py	51	RM-----APVEAYVRASSEPIYEVG-EVVYPDIIMIYHSQVTHGKS-----	YTMPFYTGKPN	103
tr_067231_067231_AQUAE_Fe	45	RM-----APVEAYVRASDQPIYEVG-EVVYPNVIMIYHPQVITHGKS-----	YTMPFYSGLKEN	97
tr_I0IRW0_I0IRW0_LEPFC_Fe	47	RL-----APVESYVRIANGKIYEIG-EIIYPNLIMIHPQVITHGKS-----	YTMPFYSGLKPN	99
tr_J9ZD37_J9ZD37_LEPFM_Py	49	RM-----APAESYVRIGPEKIYDREG-ELVYPDVVMVFMHQPVITMGKS-----	YTMPFYSGIKNN	101
tr_D3DJJ8_D3DJJ8_HYDTT_Py	47	RM-----APAESYARIGIEPIYDREG-EVVYPDVIMVFMHQPVITMGKS-----	YTMPFYSGIKNN	99
sp_P84820_PORC_THELN_Pyru	43	RG-----APVTAFTRIDDKPIRIKT-QIYEPDVVVVLDPSLLDTV-----	DVTAGLKEG	90
sp_P80907_VORA_METTM_Keto	338	RG-----GTSSCGVVISGERVGSP--AVDTPDVLFVNQPSLDE-----	FAGDVREG	382
tr_A1HTT9_A1HTT9_9FIRM_Py	44	RG-----GTANCSVISVDSDEAIGAP--IVTEPTAVVAMNLPSLDK-----	FESALLPG	88
tr_B0R3G0_B0R3G0_HALS3_Ox	46	RG-----GYTAYKVRTSVSDQVQSV--VDRLDILIALTERTVDE-----	NLDELHAD	89
tr_H3ZPH3_H3ZPH3_THELN_2-	42	RG-----GHSIAIDLISKEPIYDL--MVTKADILVALAQLGYNS-----	TKNSLREG	86
tr_Q1IQP1_Q1IQP1_KORVE_2-	49	RG-----GACSAQVVIDSKPVLYP--YVTNPDLILIVMSQEAYTK-----	FGPELKPG	93
tr_E8RJ92_E8RJ92_DESPD_2-	52	RG-----GACNAQVIISDVPIHYP--YVNTPKILVAMSQAGYDK-----	FAPALVPE	96
sp_P80906_KORC_METTM_2-ox	45	RG-----GASRAEVVISDEEIDYP--KVQSPDILVAMSHQALLT-----	YMDDLKAG	89
tr_068230_068230_HELPX_Oo	44	RG-----GPTKVDSLDRNEIIIFPYGKEGEIDFMLLSVAQISYNQ-----	FKSDIKQG	90
sp_053182_KORA_MYCTU_2-ox	70	RAPAGTLPGVSSFQIQUIADYDILTA--GDRPDVLVAMNPAAKA-----	NIGDPLG	119
tr_HODIR4_HODIR4_9STAP_2-	46	KG-----GHTNNKIRVSTSPVHAV--SDNLDILVAFQDQETIEV-----	NHHEMRAD	89
tr_087870_087870_THAAR_2-	47	RG-----GEAAAMLRLSTTPVQSH--DDHFDMLVAIDWQNVRG-----	AAEVPMTAD	92
tr_B0R4X6_B0R4X6_HALS3_Py	47	RG-----GHTYVEIRARDGTVTSR--GDGYNFLLA LGDSFARNPSEEAVYGDDEEVKPLTENLDDL RAG	107	
tr_D3DI99_D3DI99_HYDTT_2-	46	KG-----GYAQSTIRVSNNKLYYTT--GDGF DILCCFNGEAYEF-----	NRKHLRPG	89
sp_007836_IORB_THEKO_Indo	45	RF-----GSVIAYVRFGEDVY GAMV-PEGKADVILSFEPVEALR-----	YINYLKKG	90
tr_A1RYA4_A1RYA4_THEPD_In	45	RG-----GSVVVFYLKYQGPLSPIV-DQGEADVLLGELIETLR-----	RVPLLSKE	90
tr_K4MBD5_K4MBD5_9EURY_In	50	RG-----GSVNVNHIRIGCTLGSMI--SLGGADVL LALEPSEALR-----	YLDYLAED	94
sp_P80911_IORB_METTM_Indo	44	RG-----GAVSTEIRFGDVRSII--PQGEADLVIAFEPLEALR-----	ALPKMSED	88
tr_P72578_P72578_SULSP_2-	44	KG-----GHSYFSLTISDKRVRSN--TOKIDILVSFDAETVFQ-----	HFYDVVKDI	87
tr_Q96Y66_Q96Y66_SULTO_2-	44	KG-----RHSYFSLTISDKRVRSN--TOKIDILVSFDAETVFQ-----	HFYDVVKDI	87
tr_Q96XT2_Q96XT2_SULTO_2-	45	KG-----RHSYFEVVVISEKPIRSL--SSYVNILASFDAETVFQ-----	HFTETKEY	88
<u>Consensus_aa:</u>		pt.....t.s.s.h.hs...l.....shlhsh....h.....	.....hp.s	

Conservation:

sp_005650_PORC_THEME_Pyru	96	-----GILLVNTV--KDFE-----	FVRK--KTGFNGKICVVVDATDIALQEI	132
tr_M3NSB1_M3NSB1_HELPX_Py	91	-----TTYIITSY--LNKE-----	ELFEKPKELKTRKVFLVDCLKISMETL	129
tr_Q3Z8I7_Q3Z8I7_DEHM1_Py	95	-----GTLIINTT--KPLD-----	YFVS--EYGRWKIATVDATAIAKELL	131
sp_P80523_PORC_METBF_Pyru	91	-----GIIIVNTT--ENPESL-----	KLNTKARVMTVDAVKAMDII	125
sp_P80902_PORC_METTM_Pyru	91	-----GVVLLNTA--GTFT-----	SENAKIHTIDATGIALENL	121
tr_W8CQB1_W8CQB1_9EURY_Py	91	-----GMVIINTE--KSKE-----	EVLEK--LKKPAKLAVALDATTIALEIL	128
tr_Q4KY23_Q4KY23_TRIVA_Py	505	-----GVFVINFP--GSAD--LNK-----	DILPGSFRKA--IAEKDAKLYTIDATQIAIDLK	549
sp_P94692_POR_DESAF_Pyruv	508	-----GTFVLNSP--WSSLEDMDK-----	HLPMSGIKRT--IANKKLKFYNIDAVKIATDVG	554
tr_Q2RMD6_Q2RMD6_MOOTA_Py	505	-----GIFLLNST--WSA-EEMDS-----	RLPADMKR--IATKKLKFYNIDAVKIAQEIG	550
tr_C4LTX6_C4LTX6_ENTHI_Py	503	-----SVFVLNCP--WTGA-ELEA-----	QLPGSLKRV--IAEKQIKFYTIDAIGQEVK	548
sp_Q968X7_PNO_CRYPV_Pyruv	511	-----GCFVLNCP--WSTLEELNH-----	ELPSKIKHQ--IASRDVKFYVIDAQRIAQESN	557
sp_Q941N5_PNO_EUGGR_Pyruv	574	-----GTFVLNSR--WTT-EDMEK-----	EIPADFRRN--VAQKKVRFYNNVDAKICDSFG	619
tr_L8B958_L8B958_CHLRE_Py	616	-----GVLVLNTV--FTSPDSLKG-----	YLPDKVKKQ--IAALKPQLYVIDAQSVAKASG	662
sp_Q53046_NIFJ_RHORT_Pyru	516	-----ATLLLNSP--HDKD-TVWD-----	ALPRPVQQT--IIDRDLKLFWIDANKVAQETG	561
tr_B5XPH3_B5XPH3_KLEP3_Py	508	-----GTFLLNCS--WSEAE-LEQ-----	HLPVSVRRY--LAQEKFIDFTLNAVDIARELG	553
tr_Q24982_Q24982_GIAIN_Py	531	-----GFFVLNTE--HDTVETLEK-----	YLPAEMKRE--IARKNIRVYAVVNANKVAQSVG	577
tr_I2K9Y6_I2K9Y6_9PROT_Py	104	-----SLIIIINTD--FDVL-----	NEDDIKV--LEDLNATVVOFDATKLALDIA	143
tr_067231_067231_AQUAE_Fe	98	-----GMIIINS--VDII-----	PDEDKKI--LEELNAKIIYYIPATQIARDIA	137
tr_I0IRW0_I0IRW0_LEPFC_Fe	100	-----GVVLINSETPINLV-----	ADEEREL--MER-NARVYYLPATQLSREIA	140
tr_J9ZD37_J9ZD37_LEPFM_Py	102	-----GIIINDD--IELLL-----	TDSEKEE--LDQMGVLVYYYPATKMLDIA	141
tr_D3DJJ8_D3DJJ8_HYDTT_Py	100	-----GLIIINSE--EDLL-----	TDEDKEF--LESLNVKVLNFSATKFAIDIA	139
sp_P84820_PORC_THELN_Pyru	91	-----GMVIVNTE--KTKE-----	EVLEK--LKKPAKLAVALDATTIALEIL	128
sp_P80907_VORA_METTM_Keto	383	-----GIVLYDTA--TADF-----	SKKENLRAIGVPALEIAKEHG	415
tr_A1HTT9_A1HTT9_9FIRM_Py	89	-----GVLIINSS--LIERS-----	SKRDDITVYRVPANDIAELG	122
tr_B0R3G0_B0R3G0_HALS3_Ox	90	-----SIIYDGD--RTE-----	FADF--ESPAEVTLGDIPLKDLAEDAG	125
tr_H3ZPH3_H3ZPH3_THELN_2-	87	-----GLLVIDTD-----	LVKPDREYIIGAFFTRLAAEKT	115
tr_Q1IQP1_Q1IQP1_KORVE_2-	94	-----GVLIVEQD--LVKIT-----	GMSQAGRVSAPATRLAAEELG	127
tr_E8RJ92_E8RJ92_DESPD_2-	97	-----SVLLVDQD--LVN-----	PENAPCDHFIAAATRMAENLG	128
sp_P80906_KORC_METTM_2-ox	90	-----GTLIVDPD--MVIE-----	NEIQDF--VEERNISYFRAPATRTAAEKV	128
tr_068230_068230_HELPX_Oo	91	-----GIVVMDPN--LVTPTK-----	EDEEKYQLYKIPIIISIAKDEV	125
sp_053182_KORA_MYCTU_2-ox	120	-----GMVIVNSD--EFTKRNLT-----	VGYVTNPLES--GELSODYVHVTAMTTLTLGAV	167
tr_HODIR4_HODIR4_9STAP_2-	90	-----SVIIADSK--AKPDK-----	PEDCRAQMIDLFFTKTAKELG	123
tr_087870_087870_THAAR_2-	93	-----GLVLDGPD--GGE-----	FPEQ--ILAKGTRRGDIPFKKIAKEID	128
tr_B0R4X6_B0R4X6_HALS3_Py	108	-----GVIYDEG--LLDDEDV-----	GDLEQQ--ADANDWHLYPLDLRGLAKEHG	149
tr_D3DI99_D3DI99_HYDTT_2-	90	-----TVLVYDSS--DFEP-----	EEHEGVVVMYPVPLSHLAKDIM	122
sp_007836_IORB_THEKO_Indo	91	-----GLVFTNAR--PIPPVQVSMGLA-----	TYPTLDEMKKIV--EEDFGGKFMADFDEKLAMEAG	143
tr_A1RYA4_A1RYA4_THEPD_In	91	-----GVVLANNF--FLPPPAAKS-----	PSRSAVLNA--LKGLGARVVLLEADELALKAG	137
tr_K4MBD5_K4MBD5_9EURY_In	95	-----GVVIVNTE--PILPVTVTSGL-----	CSYEDVGEIMA--SLQGKRKVVGFNATQLAVEAG	145
sp_P80911_IORB_METTM_Indo	89	-----ACVIVNTS--KIPPFLNIKSP-----	HPYPPLLEEIIKT--LEENAGRVRVSFNGEKIAVEAG	140
tr_P72578_P72578_SULSP_2-	88	-----LIYNKAVETTKID--AVQSMPELAERIKDFLTKQGYETTVKGLEY--ASKNNVTLIPVNYDEIAKKVA	153	
tr_Q96Y66_Q96Y66_SULTO_2-	88	-----LIYNKAVETTKID--AVQSMPELAERIKDFLTKQGYETTVKGLEY--ASKNNVTLIPVNYDEIAKKVA	153	
tr_Q96XT2_Q96XT2_SULTO_2-	89	-----LIYNVEYENTTVD--LVKSMEPEMAEQVKEALSKERLGFTIKDVLEY--LKRRGVKVIGFNYTELICKIA	154	
<u>Consensus aa:</u>				
<u>.....thhlss.....</u>				
<u>.....phh.hsh.plt.p..</u>				

## Conservation:

		8	7	
sp_005650_PORC_THEMEA_Pyru	133	K-----RGIPNTPMLGALVRV-----TGI-VPLEAIEKRIEKMF-----KKFPQEVIDANKRALRRG		184
tr_M3NSB1_M3NSB1_HELPX_Py	130	K-----RPIPNTPMLGALMKV-----SGM-LEIEAFKEAKVVLG-----KKLTQEVIDANMLAIQRA		181
tr_Q3Z8I7_Q3Z8I7_DEHMI_Py	132	G-----VNIVNTTMLGALIKA-----TGL-AGIEDFEEPLKHRE-----KLAAKNMAAMKKA		178
sp_P80523_PORC_METBF_Pyru	126	G-----VPIVNTVLLGAFAGA-----TGE-INVESIQHAIRARFS-----GKVGEKNANAIQKA		173
sp_P80902_PORC_METTM_Pyru	122	G-----RPIVNTVMLGAFAGV-----TGL-VSIDSILIKIICKETPP-----GKIGDKNAEAARIA		169
tr_W8CQB1_W8CQB1_9EURY_Py	129	G-----LPITNTSILGAVAKA-----TGI-VKIESVEKAIKETTS-----GELGEKNAKAAREA		176
tr_Q4KY23_Q4KY23_TRIVA_Py	550	L-----PGRINNMLMQTVFFGL-----ANI-IPAECIALLKKSIAKQVARKGKEVIQKNWDMVDHA		604
sp_P94692_POR_DESAF_Pyruv	554	L-----GGRINNMIMQTAFFKL-----AGV-LPFEKAVDLLKKSIIHAYGKKGEKIVKRMNTDAVDQA		609
tr_Q2RMD6_Q2RMD6_MOOTA_Py	551	L-----GSRINVIMQTAFFKI-----ANV-IPVDEAIKYIKDSIVKTYGKKGDKILNMNFAAVDRA		605
tr_C4LTX6_C4LTX6_ENTHI_Py	549	L-----GRRINNMIMQTVFFKL-----ANV-IPFEKAIVLLKEAVQKTYGAKGPAIVKMNHDAIDKA		603
sp_Q968X7_PNO_CRYPV_Pyruv	558	L-----GRRINNLLMVMQFFSL-----TNI-IPLDLAIKLVKEAIIKKTYGKKGDAVVNSNWKAVALDT		612
sp_Q941N5_PNO_EUGGR_Pyruv	630	L-----GKRINNLMQACFFKL-----SGV-LPLAEAQRLLNESIVHEYGKKGGKVVEMNQAVNAV		674
tr_L8B958_L8B958_CHLRE_Py	663	L-----GKHVNVMVQTVFFNL-----SGV-LPMEKALALLKKSITKAYERKGPEVVAKNHSAVDMA		717
sp_Q53046_NIFJ_RHORT_Pyru	562	M-----GQRINTIMQTCFAL-----SGV-MPRDEAIEEIKKAISKTYARKSQKVIDANFAAVDQT		616
tr_B5XPH3_B5XPH3_KLEP3_Py	554	L-----GGRINNLMQAAFFKL-----TAI-IDPQTAADYLKQAVEKSYGSKGASVIEMNQRAIELG		608
tr_Q24982_Q24982_GIAIN_Py	578	L-----GGRINTIMILFFLKLGLSKLLDFDVACEDMKAARITYVA-----KQKAEVIEANVKAIDVA		634
tr_I2K9Y6_I2K9Y6_9PROT_Py	144	GT-----ELATNNAMMGMGLGL-----TKL-VTTENIEAAVKERFL-----GTSFVSSGGTAMLDSA		194
tr_067231_067231_AQUAE_Fe	138	GT-----ELATNNAMMVGTFFGI-----TRL-VTLEHIEKALIERFL-----GGTFVASGGTTALDSA		188
tr_I0IRW0_I0IRW0_LEPFC_Fe	141	DT-----DLATNNAMMVGAVSAI-----MGI-PDLPSELSQSVKERFL-----GKGFVVSGGTAALDNV		191
tr_J9ZD37_J9ZD37_LEPFM_Py	142	GT-----ELSTNMAMIGVSGL-----TDV-IGMEALDLALQDRPG-----KKYVASGGTATLDEA		191
tr_D3DJJ8_D3DJJ8_HYDTT_Py	140	GT-----ELSTNMAMIGALFGA-----VGC-VGLEAIEHGIKSRL-----KKFVASGGTASLDSA		189
sp_P84820_PORC_THELN_Pyru	129	G-----LPITNTSILGAVAKA-----TGI-VKIESVEEAIKDTTS-----GELGKKNAKAAREA		176
sp_P80907_VORA_METTM_Keto	416	T-----GRAANTAMLGVMMAL-----GITG-LDEESFRDAIRFTPS-----GKDIIIDINLKILEAG		466
tr_A1HTT9_A1HTT9_9FIRM_Py	123	N-----SKVANMVVLGALIAA-----TGA-VATTSVLKAFQKMF-----KKPELLAINEQAIHRG		172
tr_B0R3G0_B0R3G0_HALS3_Ox	126	G-----AIMRNIVALGAVCAV-----ADF-PIENLDESLEKRF-----GKGEQIIENNQKAARLG		175
tr_H3ZPH3_H3ZPH3_THELN_2-	116	GL-----ALTVNVMVALGYLVAK-----INI-VKKESEVAIRRRVP-----KGTEEINLKAFRIG		164
tr_Q1IQP1_Q1IQP1_KORVE_2-	128	K-----RMILNIVMVGFTAAV-----TNI-LQKESLREAVASSVP-----PSFRELNLKAFDRG		175
tr_E8RJ92_E8RJ92_DESPD_2-	129	N-----KMMANIIMLGFCTAI-----TKA-VSSEAAQATIRQSVP-----KGTEERNIEAFTKG		176
sp_P80906_KORC_METTM_2-ox	129	GI-----TIVANMVVMIGALTEA-----TGV-VSVRAEEEAIKNNSVP-----PGTEEKNIMAFQAG		177
tr_068230_068230_HELPX_Oo	126	GN-----IITQSVVVALAITAEF-----TKC-VEENIALDTMLKKVP-----AKVADTNKKAFEIG		174
sp_053182_KORA_MYCTU_2-ox	168	EAIGASKKDGQRAKNMFMALGLLSWM-----YGR-ELEHSAFIREKA-----RKPEIAEANVLALKAG		225
tr_HODIR4_HODIR4_9STAP_2-	124	T-----TLMKNNMVAVGATCAL-----MDL-ETETFESLITAMP-----KKGDKVVEEMNIOALHEG		173
tr_087870_087870_THAAR_2-	129	G-----GPNNMIALGTVAA-----VGL-PEDAVLVIKIDSLA-----KKGPAAALAASEASVRAG		177
tr_B0R4X6_B0R4X6_HALS3_Py	150	R-----EVMRNTAGVGATAAL-----IDM-DLDHIEDLMSDAMG-----GDILEQNLTVLRDA		196
tr_D3DI99_D3DI99_HYDTT_2-	123	KA-----YITKVNITALGVLCGL-----FDI-PVQS1KDSIKAKFL-----RKGQEIIIELNYKALETG		173
sp_007836_IORB_THEKO_Indo	144	N-----IVTTNVVNLIGALSQT-----PGFPLSEEQIKEVIRISVP-----PTKIDVNMRFAELG		192
tr_A1RYA4_A1RYA4_THEPD_In	138	S-----PITVNVMVMLGALIGT-----GRID-LTLEDADVLRSRK-----GKVLEMNLEALKLG		186
tr_K4MBD5_K4MBD5_9EURY_In	146	N-----AQAMNVIMVGAISNY-----LPL-SPD1MLDCVRELVP-----PKTVDINVKAFLFG		192
sp_P80911_IORB_METTM_Indo	141	H-----ILSLNMVMLGAAAAT-----TGFPLGEETLIESMKNNL-----PKLMEVNLRFHEG		189
tr_P72578_P72578_SULSP_2-	154	DEMKVPLSVTERVKNIVGITISYKL-----LGL-DVNYLIEAINSTPK-----QDLYRKMNELAVKDS		210
tr_Q96Y66_Q96Y66_SULTO_2-	154	DEMKVPLSVTERVKNIVGITISYKL-----LGL-DVNYLIEAINSTPK-----QDLYRKMNELAVKDS		210
tr_Q96XT2_Q96XT2_SULTO_2-	155	DTFKVPMSSVERAKMIAVGASYGL-----LGL-KFDYLKDAISSTPK-----NELFIKFNTMAELG		211
Consensus_aa:		.....Nh...shhh.h.....sh.l..p.h...hpp.h.....h.p.N..thc.t		

Cyan – Adenine binding asparagine

Green – Aromatic residues that can possibly form pi-pi interaction with adenine moiety of CoA

Magenta – Cationic residues that can possibly form cation-pi interactions with adenine moiety of CoA

Conservation:

sp_005650_PORC_THEMEA_Pyru	185	YEE--VKCSE-----	192
tr_M3NSB1_M3NSB1_HELPX_Py	182	YEE--VO-----	186
tr_Q3Z8I7_Q3Z8I7_DEHMI_Py	179	LEE--TAVKEL-KVG-----	190
sp_P80523_PORC_METBF_Pyru	174	YKL--IRGEA-----	182
sp_P80902_PORC_METTM_Pyru	170	YEK--MKHSG-----	177
tr_W8CQB1_W8CQB1_9EURY_Py	177	FEK--TVVYEL-----	185
tr_Q4KY23_Q4KY23_TRIVA_Py	605	LQG--LKEFKY-NKAEWLN--AP-----VEPRPKHE-----GIR--HIIDMSI	640
sp_P94692_POR_DESAF_Pyruv	610	VTS--LQEFKY-PDSWKDA--PAET-----KAEPMTNE-----FFK--NVVKPIL	647
tr_Q2RMD6_Q2RMD6_MOOTA_Py	606	LEA--LEEIKY-PASWADA--VDEA-----AATVTEEP-----EFIQ--KVLRPIN	644
tr_C4LTX6_C4LTX6_ENTHI_Py	604	LDG--LVEVKV-PAEWANA--PLET-----VTKIEAPE-----FVT--DVLMPLQ	641
sp_Q968X7_PNO_CRYPV_Pyruv	613	LES--LIQISYDKSQWISK--DKCGEKS-LPATAVETGNKDQEITKSTVLKQKPEHDVNQFVKDILGPVN	677
sp_Q941N5_PNO_EUGGR_Pyruv	675	FAGDLPQEVOV-PAAWANA--VDT-----TRPTGIE-----FVD--KIMRPLM	714
tr_L8B958_L8B958_CHLRE_Py	718	VAA--LKKLDI-PASWSSL--PTHVVNP-NPPAEGNTSRWE-----FIE--TVAKPML	762
sp_Q53046_NIFJ_RHORT_Pyru	617	LSR--LQSVTI-PGVLTGH--ALPP-----LVSAGAPD-----FVR--NVTAVML	654
tr_B5XPH3_B5XPH3_KLEP3_Py	609	MAA--LHRVTV-PAHWATL--EAPA-----PQASALMPD-----FIR--DILQPMN	647
tr_Q24982_Q24982_GIAIN_Py	635	RSI--IEQCHI-EYDKARW--VNADPSESTANQTYGPEPDK-----YVK--DIILPAV	680
tr_I2K9Y6_I2K9Y6_9PROT_Py	195	IEK--KFKKKE-ELLAKNM--EVIN-----	214
tr_067231_067231_AQUAE_Fe	189	IEK--KFKKKQ-ELLAKNM--EVIK-----	208
tr_I0IRW0_I0IRW0_LEPFC_Fe	192	IER--KFAKKE-QLLKKNM--EVIV-----	211
tr_J9ZD37_J9ZD37_LEPFM_Py	192	IKK--KFAKKE-MLLQKNL--DTIK-----	211
tr_D3DJJ8_D3DJJ8_HYDTT_Py	190	LER--KFKKKL-ELIEKNL--STAK-----	209
sp_P84820_PORC_THELN_Pyru	177	FEK--TVVYEL-----	185
sp_P80907_VORA_METTM_Keto	467	ADW--ARKNLE-GEF-----	478
tr_A1HTT9_A1HTT9_9FIRM_Py	173	AEC--IKK-----	178
tr_B0R3G0_B0R3G0_HALS3_Ox	176	AEY--VAEEFE-DVTLPYE--LETT-----DEDYV-----LLNGDEAIGMGA	212
tr_H3ZPH3_H3ZPH3_THELN_2-	165	YEE--GLR-----	170
tr_Q1IQP1_Q1IQP1_KORVE_2-	176	YEY--GVQALQ-TTPETGV--DENT-----VKVY-----	199
tr_E8RJ92_E8RJ92_DESPD_2-	177	FDY--GLSTLK-GREKRAA--GQTG-----AKAQ-----	200
sp_P80906_KORC_METTM_2-ox	178	REL--IMEGQK-----	186
tr_068230_068230_HELPX_Oo	175	KKH--ALEALK-K-----	184
sp_053182_KORA_MYCTU_2-ox	226	WNY--GETTEA-FGTTYEIPPAATLP-----PGEYR-----QISGNTALAYGI	264
tr_HODIR4_HODIR4_9STAP_2-	174	YRL--MOEQOLE-TVEGDFO-LTASO-----QDPHL-----YMIGNDAIGLGA	211
tr_087870_087870_THAAR_2-	178	MAF--AASLPP-SKKLAAA--AGGE-----RQRWL-----SITGNEAAGLGA	214
tr_B0R4X6_B0R4X6_HALS3_Py	197	YEQ--VSEMEH-THDLSVP--TGSH-----DEPQV-----LMSGSHAIAYGA	233
tr_D3DI99_D3DI99_HYDTT_2-	174	INY--VRENICK-LLDGYLF-PPAKE-----PKDVV-----IMEGNQAIAKGA	211
sp_007836_IORB_THEKO_Indo	193	VKA--AKEMLG-L-----	202
tr_A1RYA4_A1RYA4_THEPD_In	187	YTA--AQEQLE-GQRL-----	199
tr_K4MBD5_K4MBD5_9EURY_In	193	RAO--THV-----	198
sp_P80911_IORB_METTM_Indo	190	FET--VNCD-----	196
tr_P72578_P72578_SULSP_2-	211	YDI--VESRYN-LKPSSK-----ERRRF-----WLDGNTAVAIGK	242
tr_Q96Y66_Q96Y66_SULTO_2-	211	YDI--VESRYN-LKPSSK-----ERRRF-----WLDGNTAVAIGK	242
tr_Q96XT2_Q96XT2_SULTO_2-	212	YNS--VPNVYK-LQEYKI-----EKQRI-----QVDGNTISAMGK	243
<u>Consensus aa:</u>			
hp.....			

**Table S4. Sequences of domain III used in sequence alignment**

Number	Organism	UniProt ID
1	<i>Thermotoga maritime</i>	O05650
2	<i>Helicobacter pylori</i>	M3NSB1
3	<i>Dehalococcoides mccartyi</i>	Q3Z8I7
4	<i>Methanosarcina barkeri</i>	P80523
5	<i>Methanothermobacter marburgensis</i>	P80902
6	<i>Thermococcus guaymasensis</i>	W8CQB1
7	<i>Trichomonas vaginalis</i>	Q4KY23
8	<b><i>Desulfovibrio africanus</i></b>	P94692
9	<b><i>Moorella thermoacetica</i></b>	Q2RMD6
10	<i>Entamoeba histolytica</i>	C4LTX6
11	<i>Cryptosporidium parvum</i>	Q968X7
12	<i>Euglena gracilis</i>	Q94IN5
13	<i>Chlamydomonas reinhardtii</i>	L8B958
14	<i>Rhodospirillum rubrum</i>	Q53046
15	<i>Klebsiella pneumoniae</i>	B5XPH3
16	<i>Giardia intestinalis</i>	Q24982
29	<i>Sulfurovum sp. AR</i>	I2K9Y6
30	<i>Aquifex aeolicus</i>	O67231
31	<i>Leptospirillum ferrooxidans</i>	I0IRW0
32	<i>Leptospirillum ferriphilum</i>	J9ZD37
33	<i>Hydrogenobacter thermophiles</i>	D3DJJ8
34	<i>Thermococcus litoralis</i>	P84820
35	<i>Methanothermobacter marburgensis</i>	P80907
36	<i>Thermosinus carboxydivorans</i>	A1HTT9
37	<i>Halobacterium salinarum</i>	B0R3G0
38	<i>Thermococcus litoralis</i>	H3ZPH3
39	<i>Koribacter versatilis</i>	Q1IQP1
40	<i>Desulfovulbus propionicus</i>	E8RJ92
41	<i>Methanothermobacter marburgensis</i>	P80906
42	<i>Helicobacter pylori</i>	O68230
43	<i>Mycobacterium tuberculosis</i>	O53182
44	<i>Staphylococcus pettenkoferi</i>	H0DIR4
45	<i>Thauera aromatica</i>	O87870
46	<i>Halobacterium salinarum</i>	B0R4X6
47	<i>Hydrogenobacter thermophilus</i>	D3DI99
48	<i>Thermococcus kodakaraensis</i>	O07836
49	<i>Thermofilum pendens</i>	A1RYA4
50	<i>Methanolobus psychrophilus</i>	K4MBD5
51	<i>Methanothermobacter marburgensis</i>	P80911
52	<i>Sulfolobus sp.</i>	P72578
53	<b><i>Sulfolobus tokodaii</i></b>	Q96Y66
54	<b><i>Sulfolobus tokodaii</i></b>	Q96XT2

Cyan: “Group 3” PFOR/VOR; Purple: “Group 4” PFOR; Blue: “Group 5 PFOR/OGOR; Yellow: “Group 6” IOR; Red: “Group 7” VOR; Orange : “Group 8” OGOR.

The numbers 1-16 and 29-52 are the same as the numbers used in our previous phylogenetic analysis. Two OFORs from *Sulfolobus tokodaii* are numbered 53 and 54. Based on sequence and domain composition, two StOFORs would be classified as Group 8 OGOR.

**SI Appendix – References**

1. Menon S & Ragsdale SW (1997) Mechanism of the *Clostridium thermoaceticum* pyruvate: ferredoxin oxidoreductase: evidence for the common catalytic intermediacy of the hydroxyethylthiamine pyroporphosphate radical. *Biochemistry* 36(28):8484-8494.
2. Otwinowski Z & Minor W (1997) [20] Processing of X-ray diffraction data collected in oscillation mode. *Methods Enzymol* 276:307-326.
3. McCoy AJ, et al. (2007) Phaser crystallographic software. *J Appl Crystallogr* 40(4):658-674.
4. Adams PD, et al. (2010) PHENIX: a comprehensive Python-based system for macromolecular structure solution. *Acta Crystallogr D Biol Crystallogr* 66(2):213-221.
5. Cavazza C, et al. (2006) Flexibility of thiamine diphosphate revealed by kinetic crystallographic studies of the reaction of pyruvate-ferredoxin oxidoreductase with pyruvate. *Structure* 14(2):217-224.
6. Bunkóczki G & Read RJ (2011) Improvement of molecular-replacement models with Sculptor. *Acta Crystallogr D Biol Crystallogr* 67(4):303-312.
7. Emsley P, Lohkamp B, Scott WG, & Cowtan K (2010) Features and development of Coot. *Acta Crystallogr D Biol Crystallogr* 66(4):486-501.
8. Kung Y, Doukov TI, Seravalli J, Ragsdale SW, & Drennan CL (2009) Crystallographic snapshots of cyanide-and water-bound C-clusters from bifunctional carbon monoxide dehydrogenase/acetyl-CoA synthase. *Biochemistry* 48(31):7432-7440.
9. Kutter S, et al. (2009) Covalently bound substrate at the regulatory site of yeast pyruvate decarboxylases triggers allosteric enzyme activation. *J Biol Chem* 284(18):12136-12144.
10. Agarwal V, Metlitskaya A, Severinov K, & Nair SK (2011) Structural basis for microcin C7 inactivation by the MccE acetyltransferase. *J Biol Chem* 286(24):21295-21303.
11. Hariharan PC & Pople JA (1973) The influence of polarization functions on molecular orbital hydrogenation energies. *Theoret Chim Acta* 28(3):213-222.
12. Lee C, Yang W, & Parr R (1988) Density-functional exchange-energy approximation with correct asymptotic behaviour. *Phys Rev B* 37:785-789.
13. Becke AD (1993) Becke's three parameter hybrid method using the LYP correlation functional. *J Chem Phys* 98:5648-5652.
14. Frisch M, et al. (2008) Gaussian 03, revision C. 02 (Gaussian Inc.).
15. Morin A, et al. (2013) Cutting edge: Collaboration gets the most out of software. *eLife* 2:e01456.
16. Gibson MI, Chen PY-T, & Drennan CL (2016) A structural phylogeny for understanding 2-oxoacid oxidoreductase function. *Curr Opin Struct Biol* 41:54-61.
17. Pei J, Kim B-H, & Grishin NV (2008) PROMALS3D: a tool for multiple protein sequence and structure alignments. *Nucleic Acids Res* 36(7):2295-2300.
18. Gibson MI, et al. (2015) The structure of an oxalate oxidoreductase provides insight into microbial 2-oxoacid metabolism. *Biochemistry* 54(26):4112-4120.
19. Yan Z, Maruyama A, Arakawa T, Fushinobu S, & Wakagi T (2016) Crystal structures of archaeal 2-oxoacid: ferredoxin oxidoreductases from *Sulfolobus tokodaii*. *Sci Rep* 6:33061.
20. Gibson MI, et al. (2016) One-carbon chemistry of oxalate oxidoreductase captured by X-ray crystallography. *Proc Natl Acad Sci USA* 113(2):320-325.
21. Furdui C & Ragsdale SW (2002) The roles of coenzyme A in the pyruvate: ferredoxin oxidoreductase reaction mechanism: rate enhancement of electron transfer from a radical intermediate to an iron-sulfur cluster. *Biochemistry* 41(31):9921-9937.
22. Mansoorabadi SO, et al. (2006) EPR spectroscopic and computational characterization of the hydroxyethylidene-thiamine pyrophosphate radical intermediate of pyruvate: ferredoxin oxidoreductase. *Biochemistry* 45(23):7122-7131.
23. Reed GH, Ragsdale SW, & Mansoorabadi SO (2012) Radical reactions of thiamin pyrophosphate in 2-oxoacid oxidoreductases. *BBA Proteins Proteomics* 1824(11):1291-1298.
24. Pierce E, Mansoorabadi SO, Can M, Reed GH, & Ragsdale SW (2017) Properties of intermediates in the catalytic cycle of oxalate oxidoreductase and its suicide inactivation by pyruvate. *Biochemistry* 56(22):2824-2835.